Electronic Supplementary Material (ESI) for Materials Horizons.

A supramolecular approach for converting renewable biomass into functional materials

Yunfei Zhang[a], Changyong Cai[a], Ke Xu[b], Xiao Yang[c], Leixiao Yu[b*], Lingyan Gao[c*], & Shengyi Dong[a*]

[a]College of Chemistry and Chemical Engineering, Hunan University, Changsha 410082, China

[b]State Key Laboratory of Oral Diseases, National Clinical Research Center for Oral Diseases, West China Hospital of Stomatology, Sichuan University, 610064 Chengdu, China

[c]Key Laboratory of Synthetic and Natural Functional Molecule Chemistry of the Ministry of Education, College of Chemistry & Materials Science, Northwest University, 710069 Xi'an, China

*Corresponding author. E-mail: dongsy@hnu.edu.cn; leixiaoyu@scu.edu.cn, gaolingyan@nwu.edu.cn.

Table of Contents

1. Materials and methods 3
2. The preparation and characterization of poly[**TA-biomass**]s 5
3. Thermogravimetric analysis(TGA) of poly[**TA-biomass**]s 11
4. FT-IR spectra of poly[**TA-biomass**]s 12
5. The stability and processability of poly[**TA-biomass**]s 12
6. Adhesion behavior of poly[**TA-biomass**]s 15
7. Mechanical properties of poly[**TA-biomass**]s 17
8. Impact resistance of poly[**TA-biomass**]s 20
9. The recyclability of poly[**TA-biomass**]s 22
10. The biocompatibility and antibacterial properties of poly[**TA-biomass**]s 23
11. Videos 30
12. References 31

1. Materials and methods

DL-thioctic acid (**TA**) was purchased from Shanghai Aladdin Biochemical Technology Co., Ltd (Shanghai, China). Cellulose (**Ce**), sericin protein (**Sp**), chitin (**Ch**), guar gum (**Gu**), corn protein (**Cp**), and potato starch (**Ps**) were purchased from Shanghai Macklin Biochemical Technology Co., Ltd. Other solvents and materials were commercially obtained and used directly. ^{1}H NMR spectra were collected on a Bruker-AV400 with TMS as the internal standard. Infrared (IR) spectra were collected on a Thermo Scientific Nicolet iS10 FT-IR spectrometer. Dynamic thermomechanical analyses (DMA) were performed on a DMA 8000-PerkinElmer using shear model. Thermogravimetric analysis (TGA) was carried out using a TG 5500, and the heating rate was 20 ºC min^{-1} from 30 to 600 ºC in nitrogen atmosphere. Scanning electron microscopy (SEM) images were collected on Sigma 300. Atomic force microscope (AFM) images were collected on Bruker. Rheology measurements were performed on an Anton Paar MCR 92. The laminator model PP15 was chosen with 15 mm of diameter and 1 mm of gap. The adhesion strength measurements were performed on a HY-0580 Electronic tensile testing machine. The rebound rate of falling ball is measured by ASR-3010 instrument (ISO 8307: 2007, MOD). Impact resistance is measured by digital impact tester XBL instrument (GB/T1043-2008).

Gram-negative bacterial strain *Escherichia coli* (*E. coli*, ATCC25922), Gram-positive bacterial strain *Staphylococcus aureus* (ATCC25923) and methicillin-resistant *Staphylococcus aureus* (ATCC 43300) were adopted in this study. The bacteria were initially streaked from –80 °C glycerol stocks on lysogeny broth (LB or TSB). After growth on LB or TSB agar plates, the cells were cultured from a fresh single colony in LB or TSB. All experiments were conducted at 37 °C. All glassware used in this study was sterilized before test.

Preparation of poly[TA]

TA powder (and additives) was heated at 120 °C for 2 hours.[S1]

Antibacterial activity

E. coli and *S. aureus* bacterial suspension used in the antibacterial test were 10^5

CFU/mL in phosphate buffered saline (PBS), respectively (CFU represents for colony forming units). First, the bulk materials with different additives were placed into a standard 96-well culture plate (10 mg per well). Then 200 μL of corresponding bacterial suspension was added into each well. After that, the cultures and the samples were incubated in an incubator at 37 °C for 24 h. 100 μL of planktonic bacterial suspensions were then serially diluted and added onto the nutrition agar plates, respectively. The bacterial colonies were recorded after incubation at 37 °C for 24 h. Each experiment was repeated three times.

Propidium iodide (PI) uptake assay. Cell membrane permeability assays with the propidium iodide (PI) probe were performed according to the literature.[S2] Bacterial suspension of *E. coli* or *S. aureus* (OD_{600} = 0.34) was prepared to carry out the PI assay. 180 μL of the bacterial suspension was transferred into the wells of a 96-well plate and incubated with poly[**TA-biomass**]s for 90 min. Then, poly[**TA-biomass**]s were removed from the bacterial suspension and PI dye (400 μM, 20 μL) was added into the wells containing *E. coli* or *S. aureus* bacterial suspension and further incubated for 20 min. Changes in fluorescence were monitored by a microplate reader (Thermo Scientific TY2015000747). Triton X-100 (1%) in PBS was used as the positive control and pure PBS was used as the negative control, respectively.

DNA and protein leakage assays. *E. coli* and *S. aureus* bacterial suspensions were treated with **TA** and poly[**TA**], respectively, for 90 min. Then, these aqueous suspensions of bacterial cells were centrifuged, filtered with a membrane (0.22 μm), and the supernatants were collected. *E. coli* and *S. aureus* cells with 1% TritonX-100 and PBS buffer were used as the positive and negative control, respectively. DNA concentrations were quantified by measuring the optical values of the collected supernatants at the wavelength of 260 nm (OD_{260}). The protein contents in the supernatants were measured using an enhanced BCA protein assay kit. The absorbance intensity at 562 nm was recorded by a microplate reader (Thermo Scientific TY2015000747) and the protein concentrations were calculated against a standard calibration curve using bovine serum albumin (BSA) as a model protein.

2. The preparation and characterization of poly[TA-biomass]s

Table S1. Density of poly[**TA-biomass**]s.

Poly[**TA-biomass**]s	Density (g/cm^3)
poly[**TA-Ce**]	1.468
poly[**TA-Sp**]	1.407
poly[**TA-Ch**]	1.319
poly[**TA-Gu**]	1.628
poly[**TA-Ps**]	1.381
poly[**TA-Cp**]	1.323

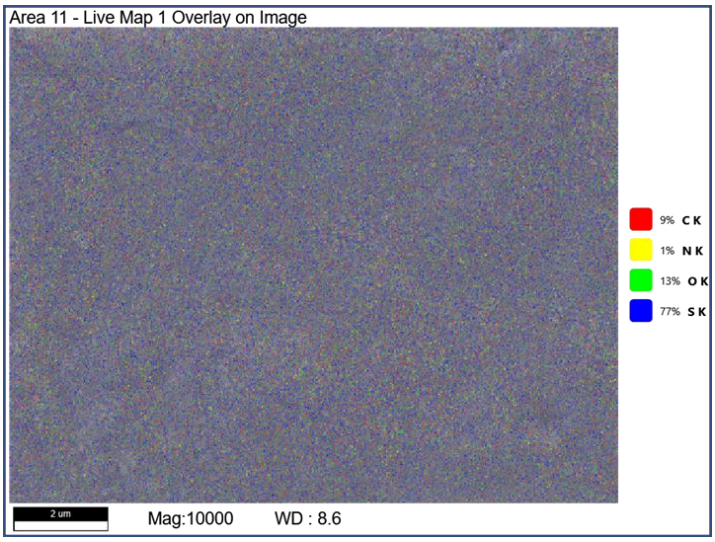

Figure S1. EDS (mapping) image of poly[**TA-Ch**] (**TA/Ch** = 10/1).

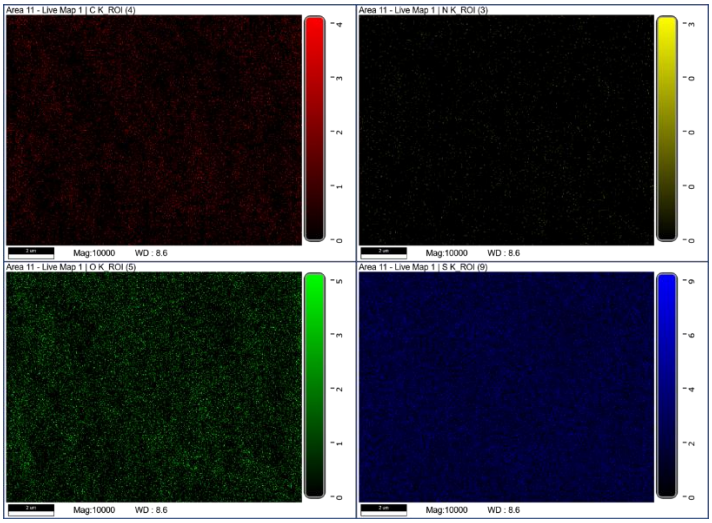

Figure S2. EDS (mapping) images (C, N, O, and S) of poly[**TA-Ch**].

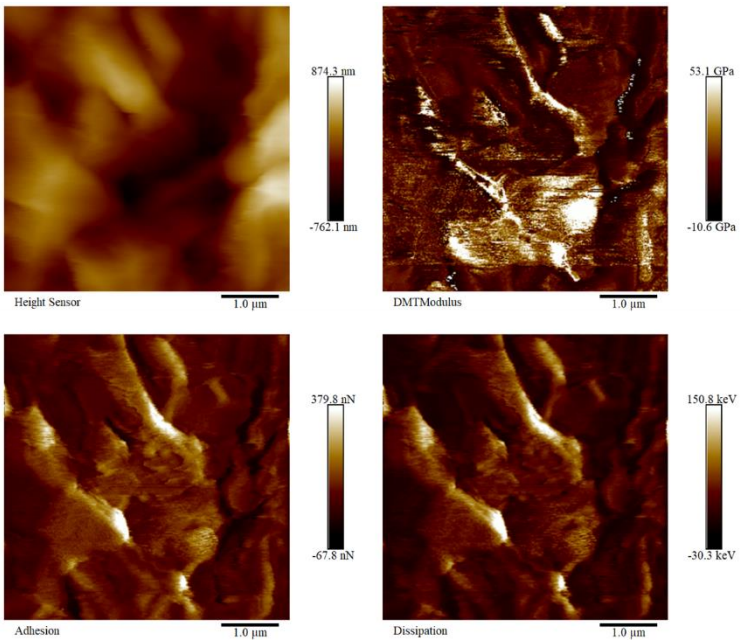

Figure S3. AFM of poly[**TA-Ce**] (**TA/Ce** = 10/1).

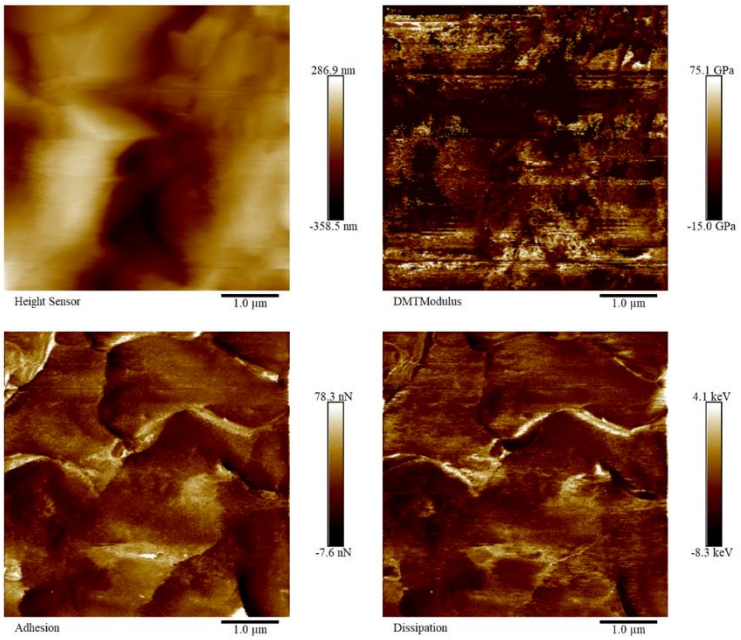

Figure S4. AFM of poly[**TA-Sp**] (**TA/Ch** = 10/1).

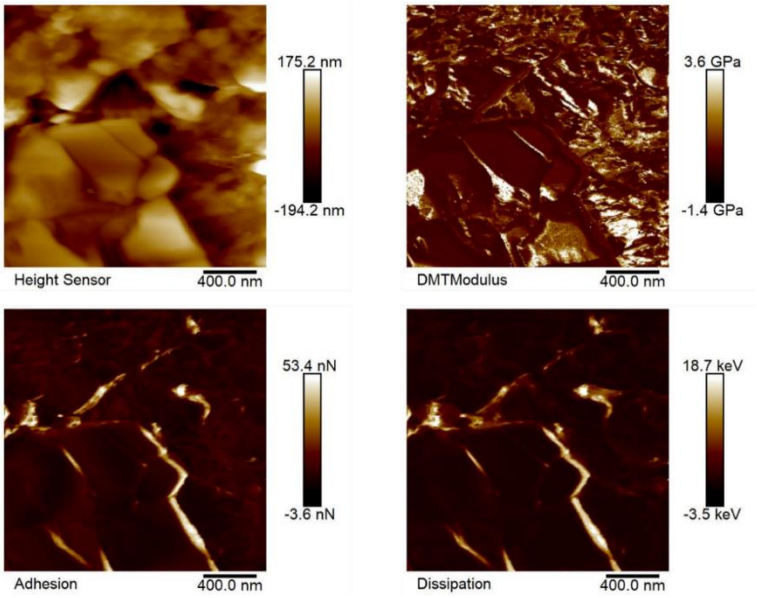

Figure S5. AFM of poly[**TA-Ch**] (**TA/Ch** = 10/1).

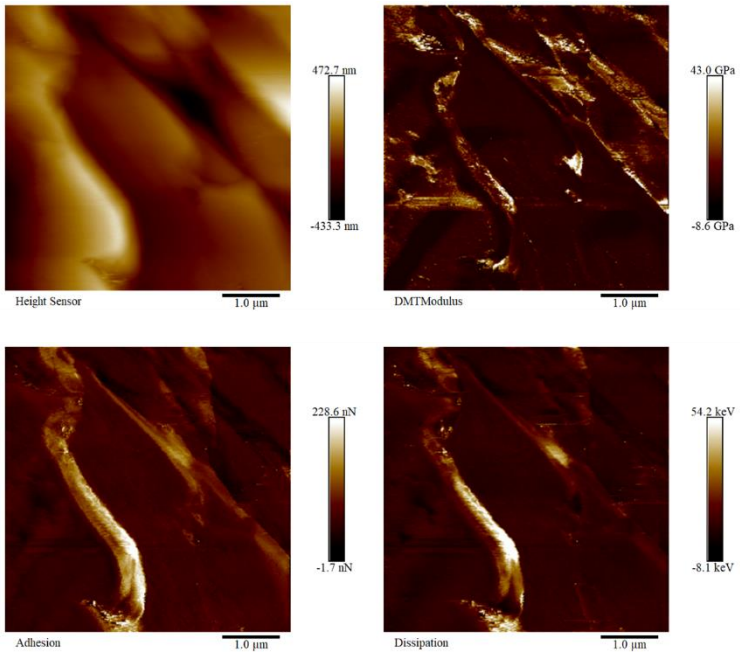

Figure S6. AFM of poly[**TA-Gu**] (**TA/Gu** = 10/1).

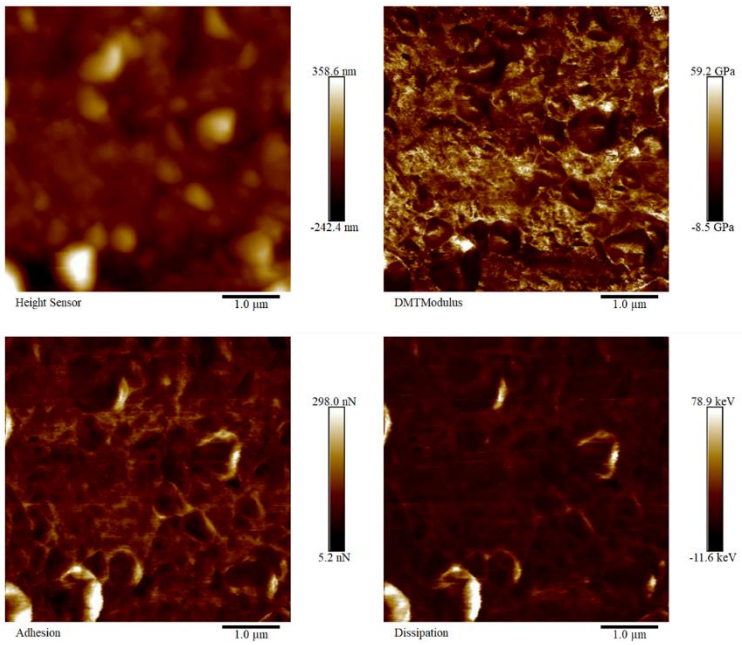

Figure S7. AFM of poly[**TA-Cp**] (**TA**/**Cp** = 10/1).

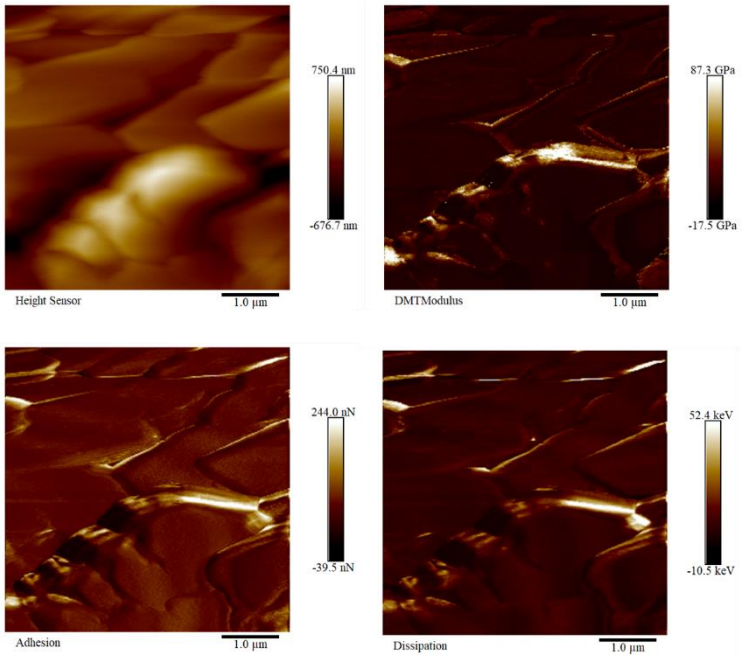

Figure S8. AFM of poly[**TA-Ps**] (**TA**/**Ps** = 10/1).

As shown in these AFM images, poly[**TA-biomass**]s have high values of DMT moduli, demonstrating their good rigidities in microscopic view.

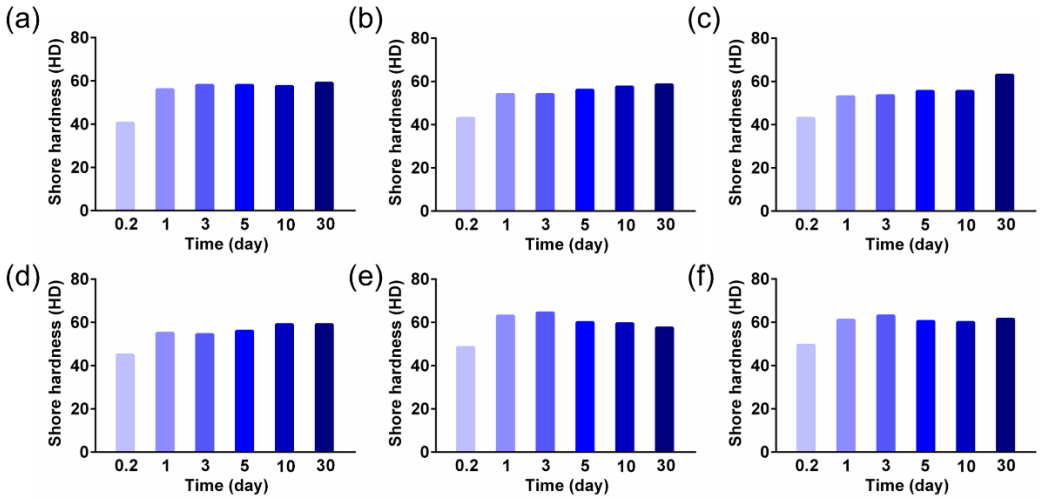

Figure S9. Time-dependent Shore hardness (Shore D) of poly[**TA-biomass**]s (25 ºC, **TA/biomass** = 10/1): (a) poly[**TA-Ce**]; (b) poly[**TA-Sp**]; (c) poly[**TA-Ch**]; (d) poly[**TA-Gu**]; (e) poly[**TA-Cp**]; and (f) poly[**TA-Ps**].

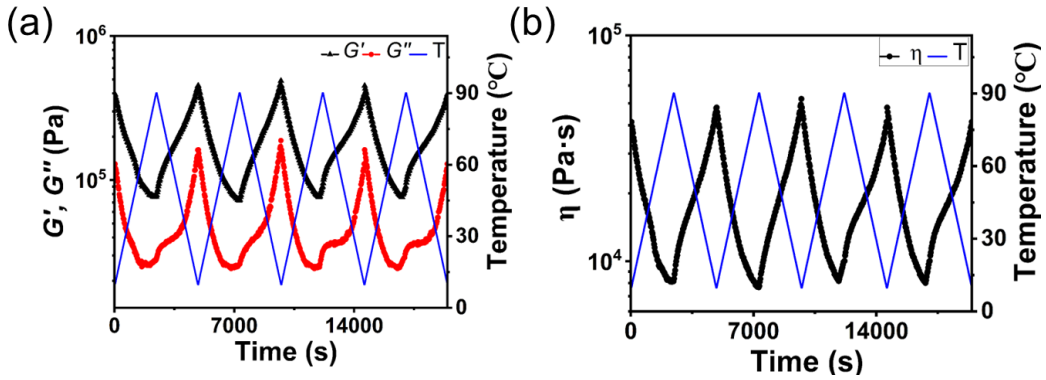

Figure S10. Storage (*G'*), loss (*G''*) moduli and viscosity (η) of poly[**TA-Sp**] at reversible temperature-dependent rheological tests.

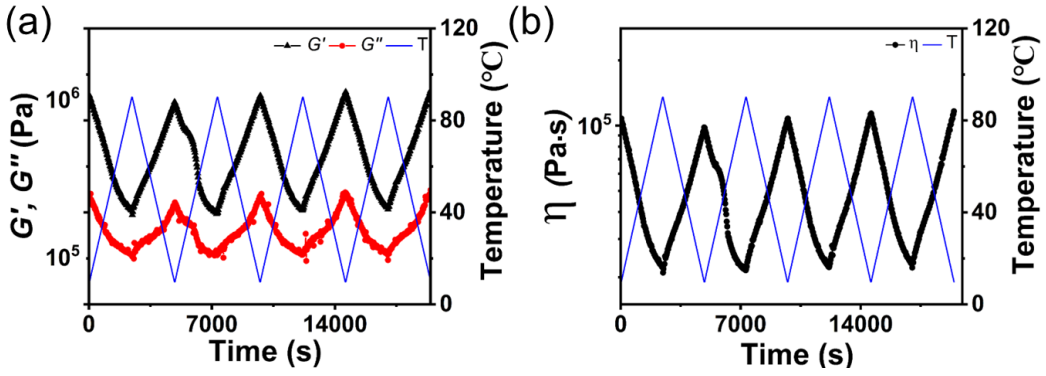

Figure S11. Storage (*G'*), loss (*G''*) moduli and viscosity (η) of poly[**TA-Ch**] at reversible temperature-dependent rheological tests.

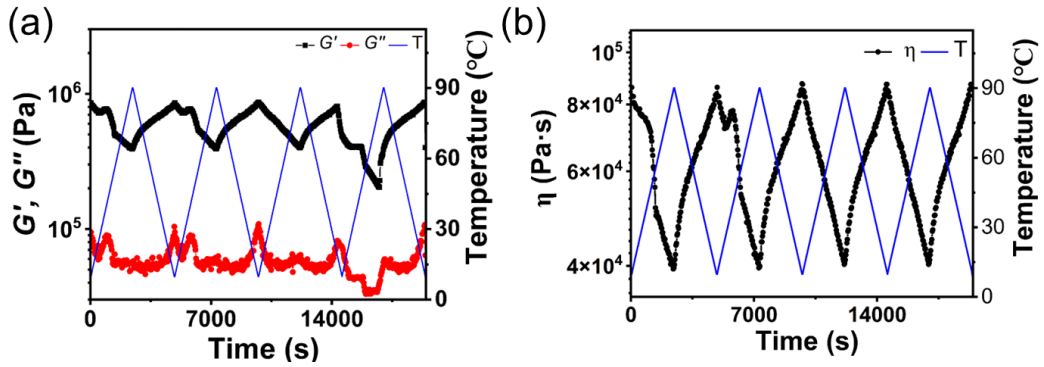

Figure S12. Storage (*G'*), loss (*G''*) moduli and viscosity (η) of poly[**TA-Gu**] at reversible temperature-dependent rheological tests.

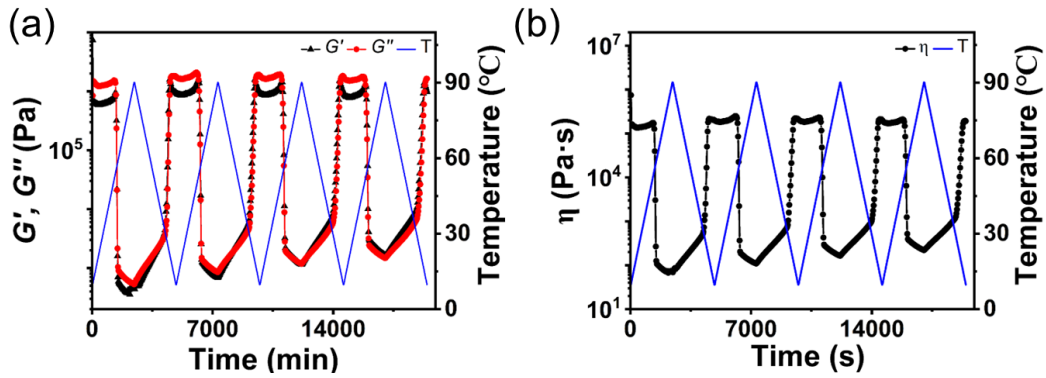

Figure S13. Storage (*G'*), loss (*G''*) moduli and viscosity (η) of poly[**TA-Cp**] at reversible temperature-dependent rheological tests.

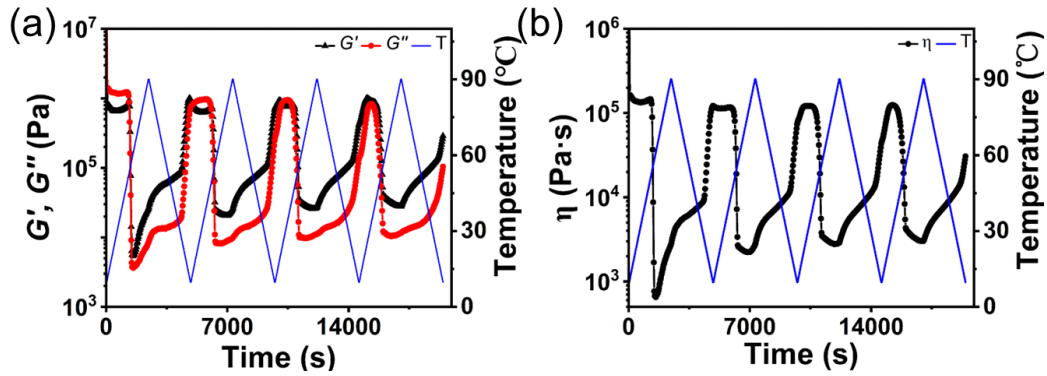

Figure S14. Storage (*G'*), loss (*G''*) moduli and viscosity (η) of poly[**TA-Ps**] at reversible temperature-dependent rheological tests.

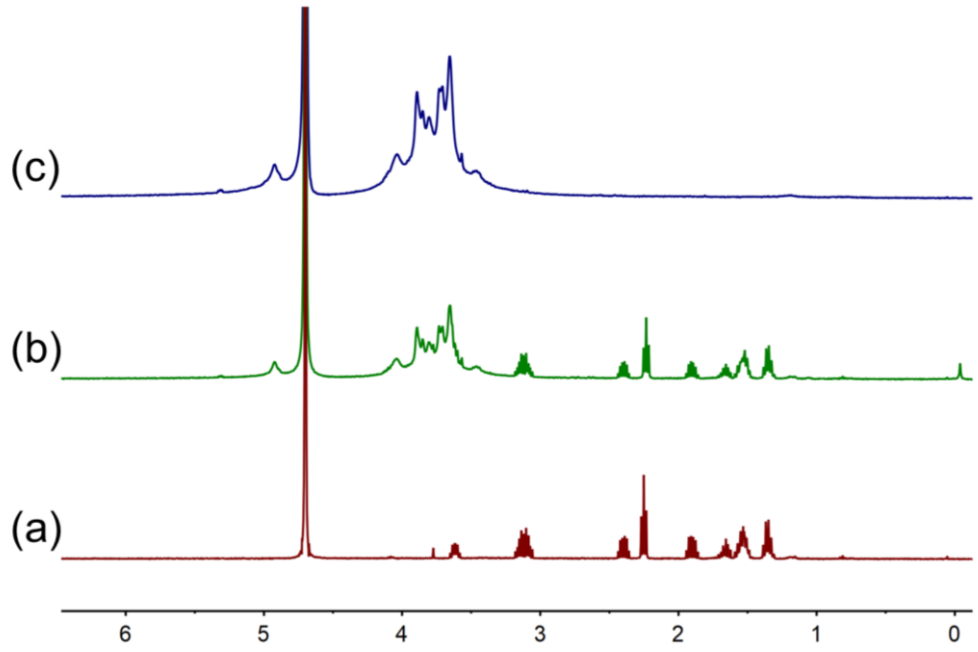

Figure S15. ^{1}H NMR (400 MHz, D_2O, room temperature): (a) **TA**, (b) **TA-Gu**, and (c) **Gu**.

3. Thermogravimetric analysis(TGA) of poly[TA-biomass]s

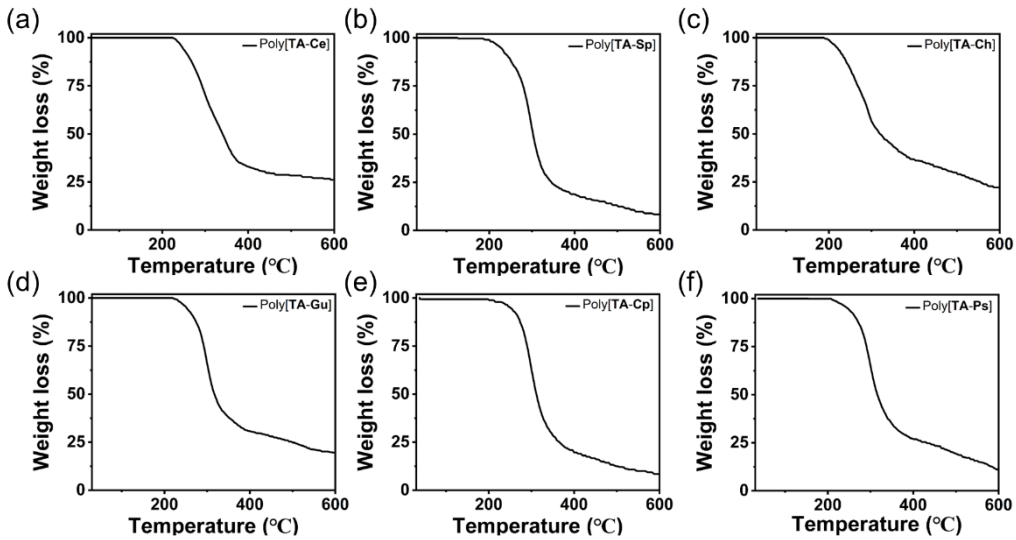

Figure S16. TGA spectra of (a) poly[**TA-Ce**]; (b) poly[**TA-Sp**]; (c) poly[**TA-Ch**]; (d) poly[**TA-Gu**]; (e) poly[**TA-Cp**]; and (f) poly[**TA-Ps**].

These results demonstrate that poly[**TA-biomass**]s have good thermal stability.

4. FT-IR spectra of poly[TA-biomass]s

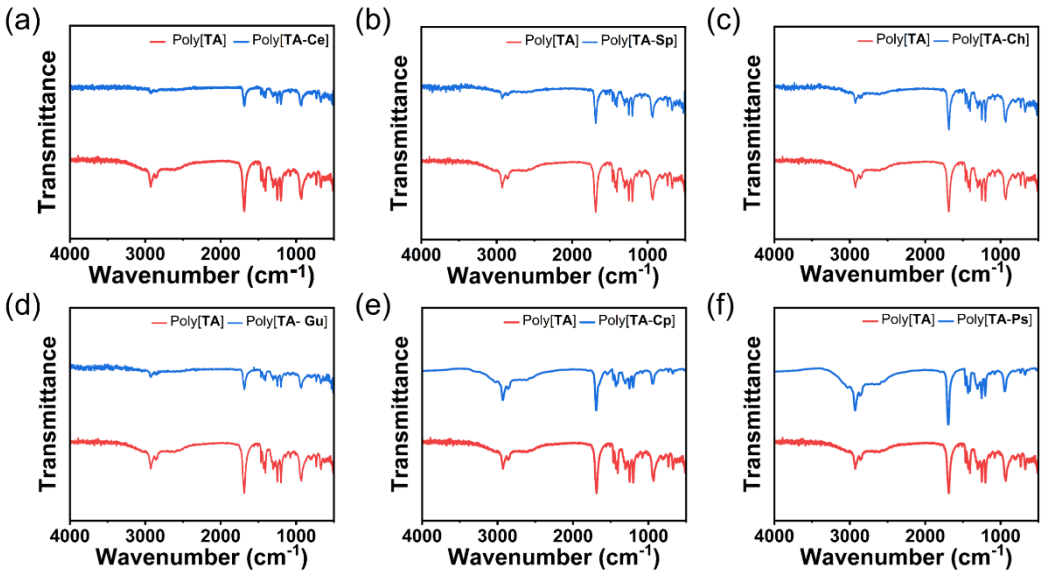

Figure S17. FT-IR spectra of (a) poly[**TA-Ce**]; (b) poly[**TA-Sp**]; (c) poly[**TA-Ch**]; (d) poly[**TA-Gu**]; (e) poly[**TA-Cp**]; and (f) poly[**TA-Ps**].

5. The stability and processability of poly[TA-biomass]s

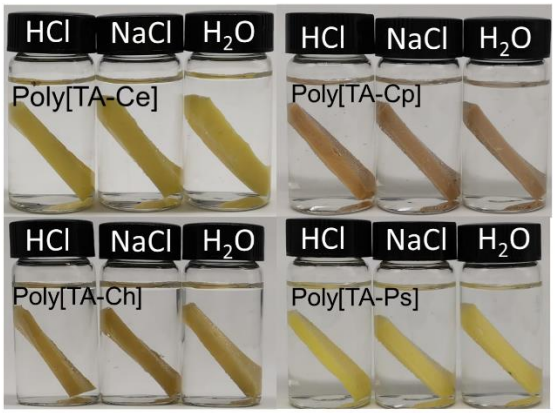

Figure S18. Stability of poly[**TA-Ce**], poly[**TA-Ch**], poly[**TA-Cp**], and poly[**TA-Ps**] at different conditions: HCl (0.5 M), NaCl (2.8 wt%), H_2O (6 months).

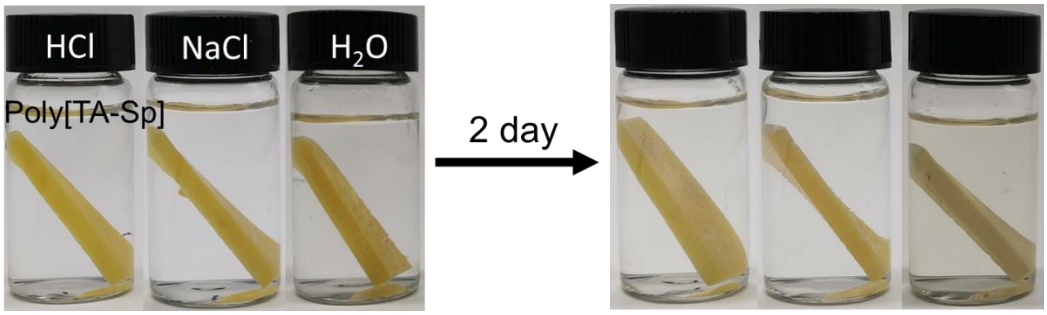

Figure S19. Stability of poly[**TA-Sp**] at different conditions: HCl (0.5 M), NaCl (2.8 wt%), H_2O.

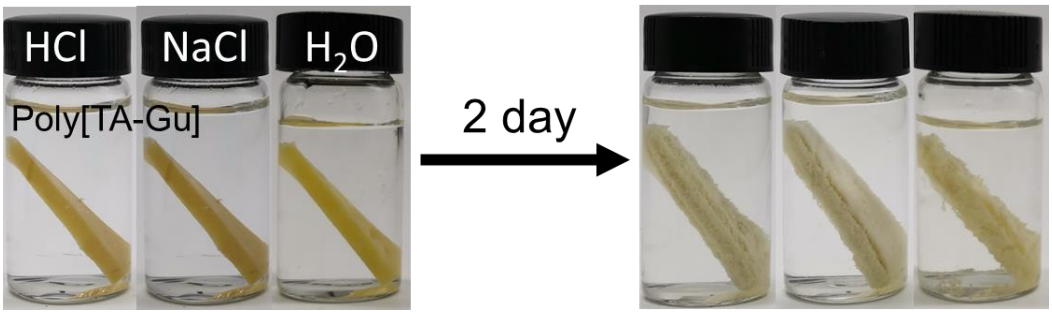

Figure S20. Stability of poly[**TA-Gu**] at different conditions: HCl (0.5 M), NaCl (2.8 wt%), H_2O.

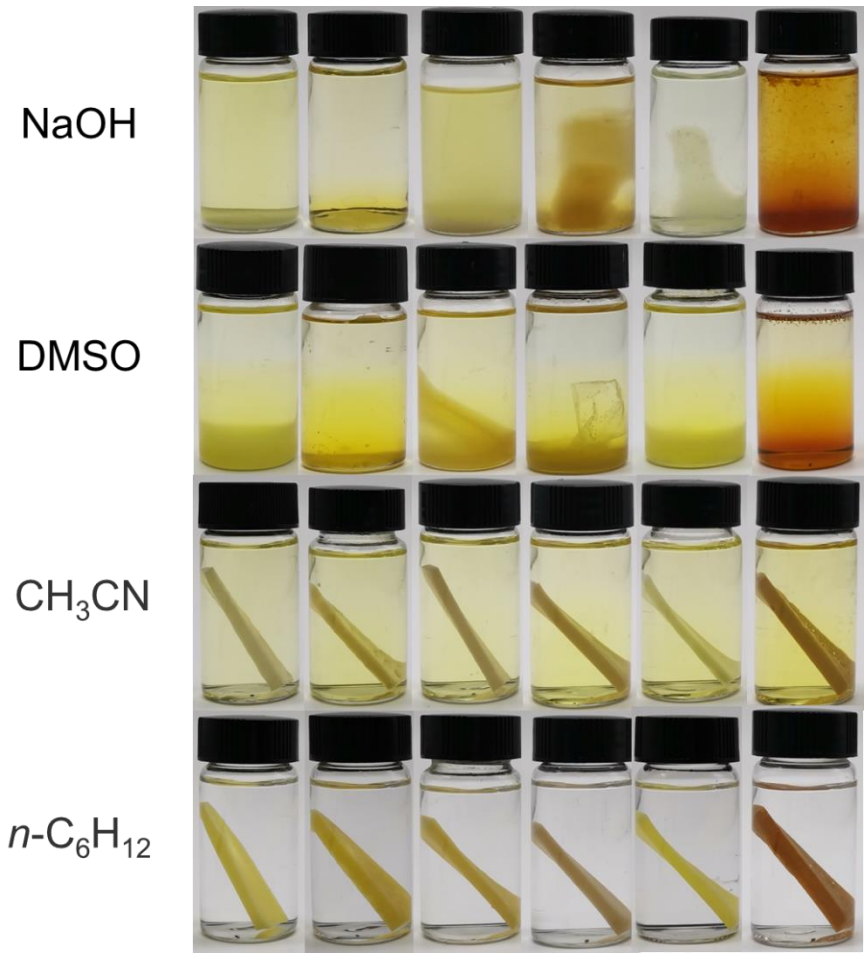

Figure S21. Stability of poly[**TA-biomass**]s at different conditions after 1 day: NaOH (1 M), DMSO, CH_3CN, and *n*-hexane (From left to right are poly[**TA-Ce**], poly[**TA-Sp**], poly[**TA-Ch**], poly[**TA-Gu**], poly[**TA-Cp**], and poly[**TA-Ps**]).

The stability of poly[**TA-biomass**]s under basic solution and organic solvents,

including sodium hydroxide solution, DMSO, CH_3CN, and *n*-hexane, were added (Figure S21). It was found that poly[**TA-biomass**]s are not stable in basic solution, because of the carboxyl acid groups in **TA**. Meanwhile, different phenomena were recorded, when poly[**TA-biomass**]s were immersed in organic solvents. Poly[**TA-biomass**]s are stable in acetonitrile and hexane.

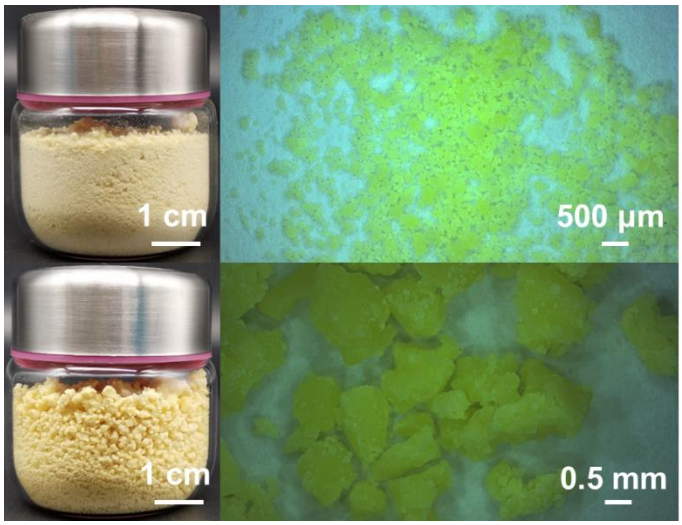

Figure S22. Photos of poly[**TA-Ch**].

Figure S23. Poly[**TA-Ce**] film. (the thickness of film is 0.09 mm; **TA/Ce** = 10/1)

Figure S24. Poly[**TA-Ce**] models. (**TA/Ce** = 10/1)

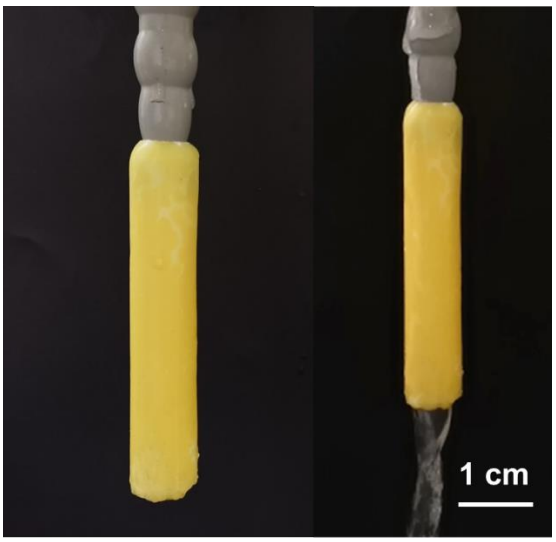

Figure S25. Poly[**TA-Ce**] water pipe models. (**TA**: **Ce** = 10: 1)

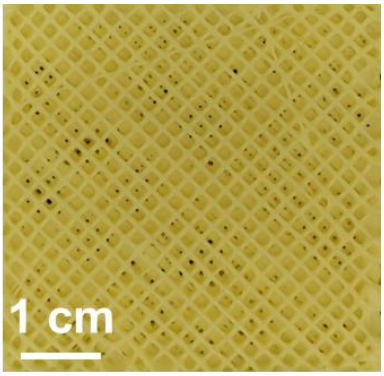

Figure S26. 3D printed poly[**TA-Ce**] model. (**TA/Ce** = 10/1)

6. Adhesion behavior of poly[TA-biomass]s

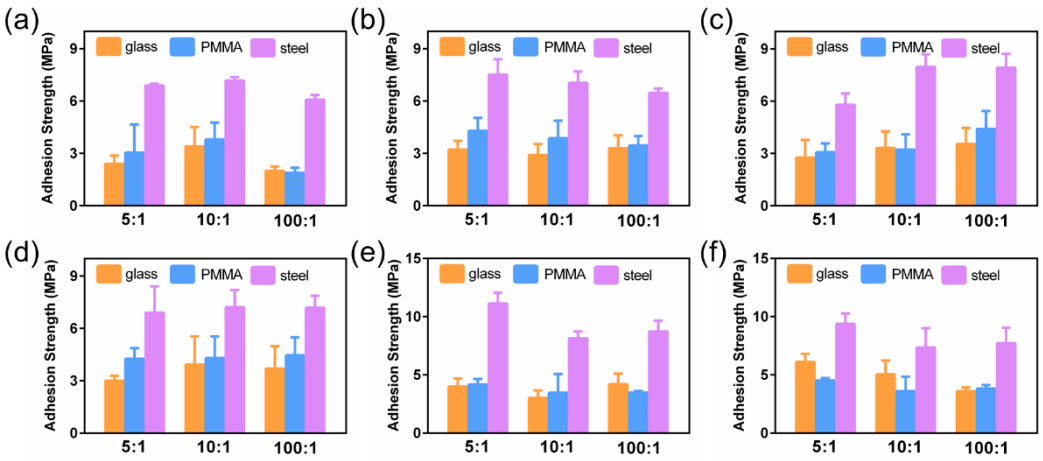

Figure S27. The adhesion strengths of poly[**TA-biomass**]s (25 ºC): (a) poly[**TA-Ce**]; (b) poly[**TA-Sp**]; (c) poly[**TA-Ch**]; (d) poly[**TA-Gu**]; (e) poly[**TA-Cp**]; and (f) poly[**TA-Ps**].

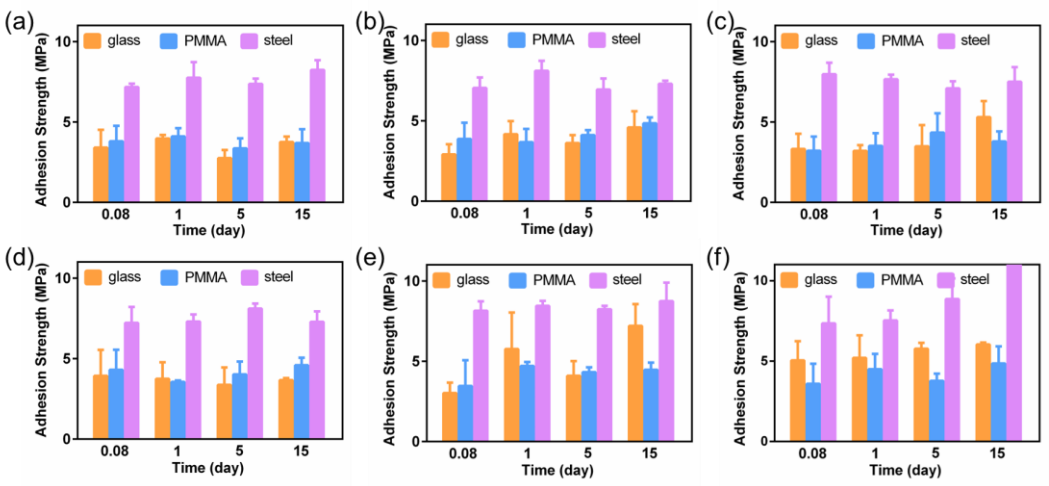

Figure S28. Time-dependent adhesion strengths of poly[**TA-biomass**]s (25 ºC, **TA/biomass** = 10/1): (a) poly[**TA-Ce**]; (b) poly[**TA-Sp**]; (c) poly[**TA-Ch**]; (d) poly[**TA-Gu**]; (e) poly[**TA-Cp**]; and (f) poly[**TA-Ps**].

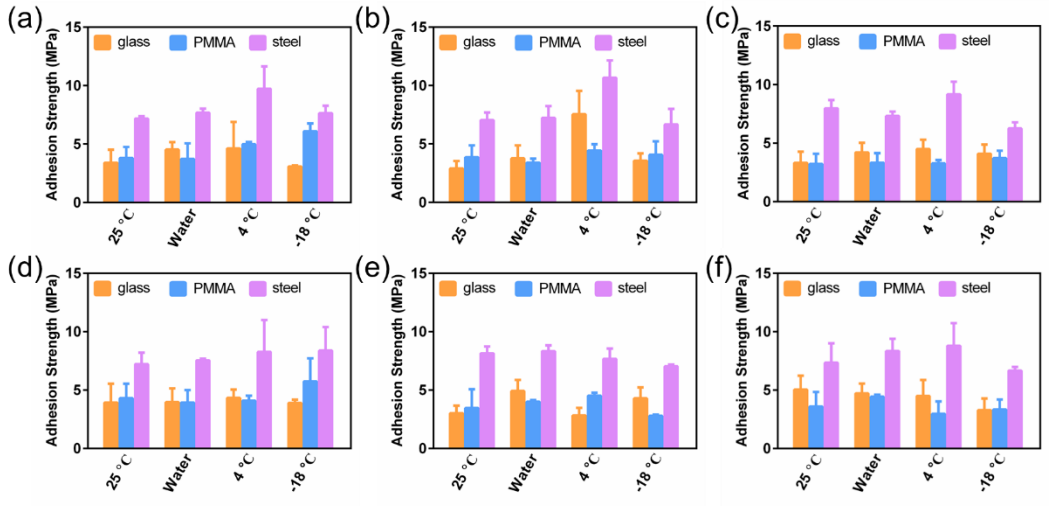

Figure S29. Adhesion strengths of poly[**TA-biomass**]s at different conditions (**TA/biomass** = 10/1): (a) poly[**TA-Ce**]; (b) poly[**TA-Sp**]; (c) poly[**TA-Ch**]; (d) poly[**TA-Gu**]; (e) poly[**TA-Cp**]; and (f) poly[**TA-Ps**].

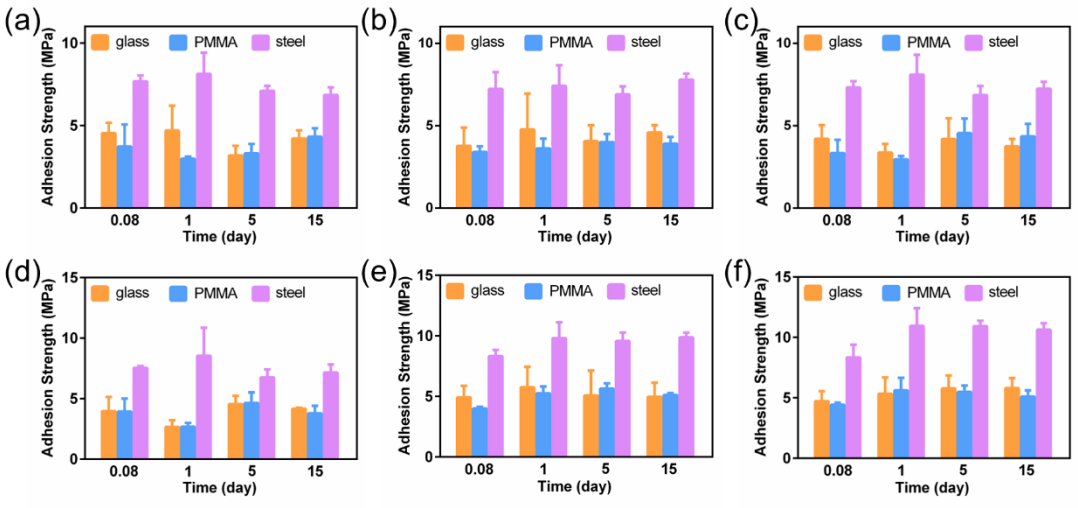

Figure S30. Time-dependent underwater adhesion strengths of poly[**TA-biomass**]s (**TA**/**biomass** = 10/1): (a) poly[**TA-Ce**]; (b) poly[**TA-Sp**]; (c) poly[**TA-Ch**]; (d) poly[**TA-Gu**]; (e) poly[**TA-Cp**]; and (f) poly[**TA-Ps**].

7. Mechanical properties of poly[TA-biomass]s

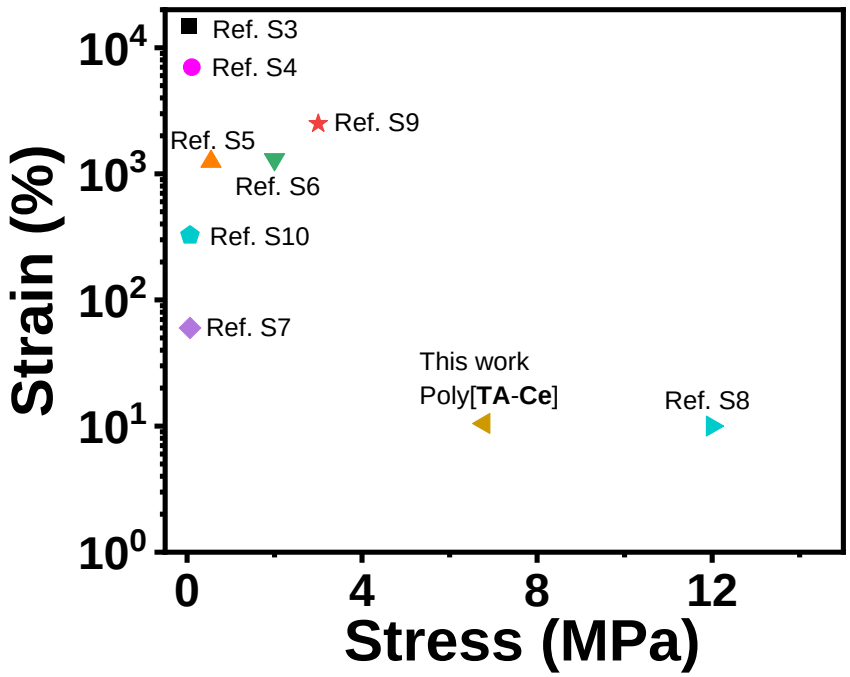

Figure S31. Comparison of our work and reported **TA**-based materials with different functions.

Table S2. Comparison of our work and reported **TA**-based materials.

Reference	Transparent	Stretchability	State
Ref.3	yes	yes	soft
Ref.4	yes	yes	soft
Ref.5	no	yes	soft
Ref.6	yes	yes	soft
Ref.7	no	yes	soft
Ref.8	yes	no	hard
Ref.9	yes	yes	soft
Ref.10	yes	yes	soft
This work	no	no	hard

Figure S32. The photo of poly[**TA-Ch**] long-term weight-loading tests.

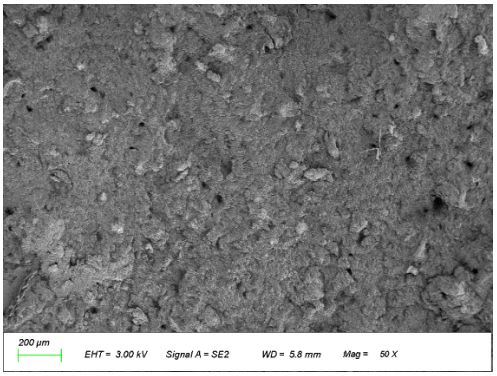

Figure S33. SEM image of poly[**TA-Ch**] fracture surface.

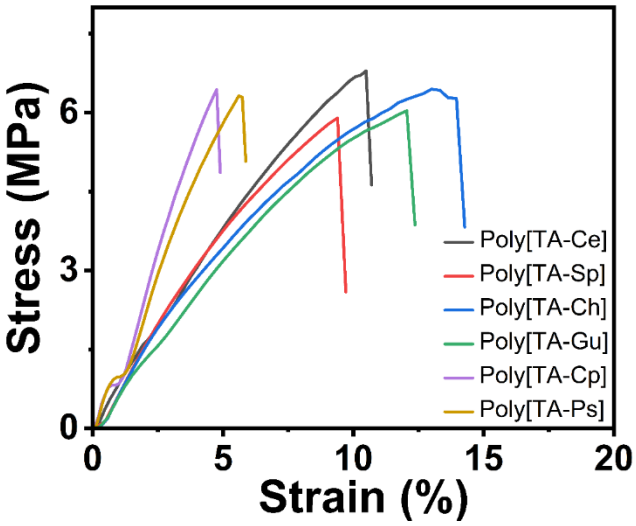

Figure S34. Strain-stress curves of poly[**TA-biomass**]s. (**TA/biomass** = 10/1)

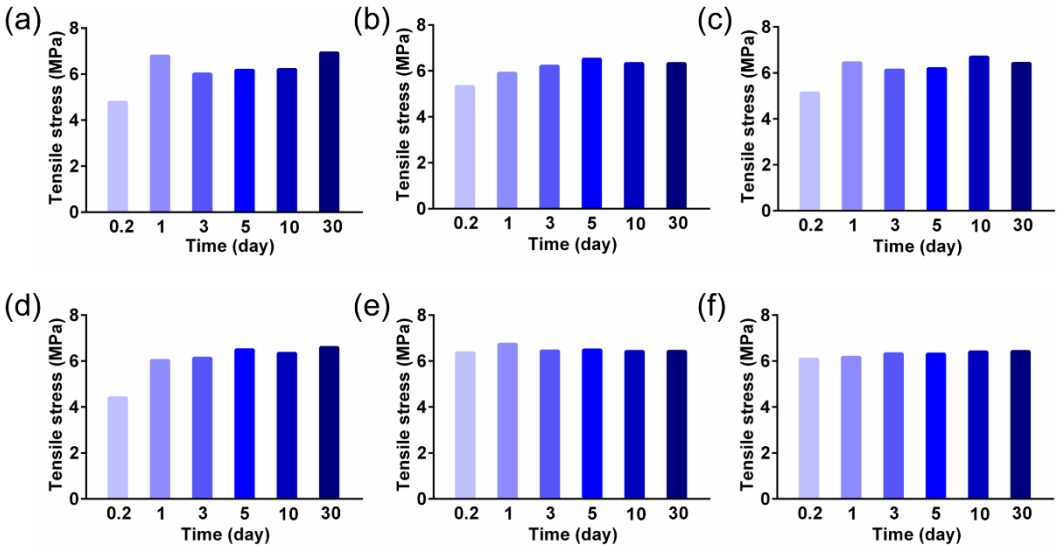

Figure S35. Time-dependent tensile strengths of poly[**TA-biomass**]s (25 ºC, **TA/biomass** = 10/1): (a) poly[**TA-Ce**]; (b) poly[**TA-Sp**]; (c) poly[**TA-Ch**]; (d) poly[**TA-Gu**]; (e) poly[**TA-Cp**]; and (f) poly[**TA-Ps**].

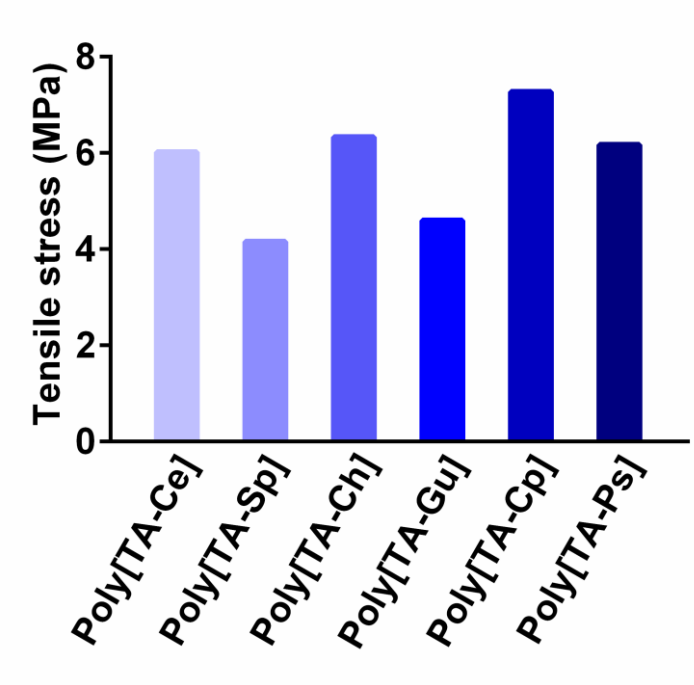

Figure S36. Tensile strengths of poly[**TA-biomass**]s under water. (**TA/biomass** = 10/1)

8. Impact resistance of poly[TA-biomass]s

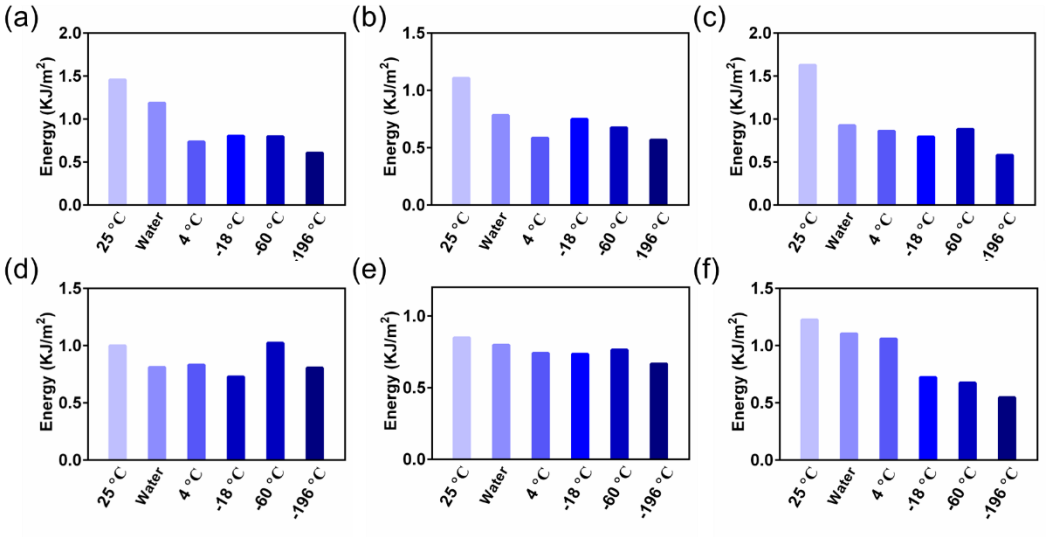

Figure S37. Impact resistance of poly[**TA-biomass**]s at different conditions (**TA/biomass** = 10/1): (a) poly[**TA-Ce**]; (b) poly[**TA-Sp**]; (c) poly[**TA-Ch**]; (d) poly[**TA-Gu**]; (e) poly[**TA-Cp**]; and (f) poly[**TA-Ps**].

Figure S38. Ce film.

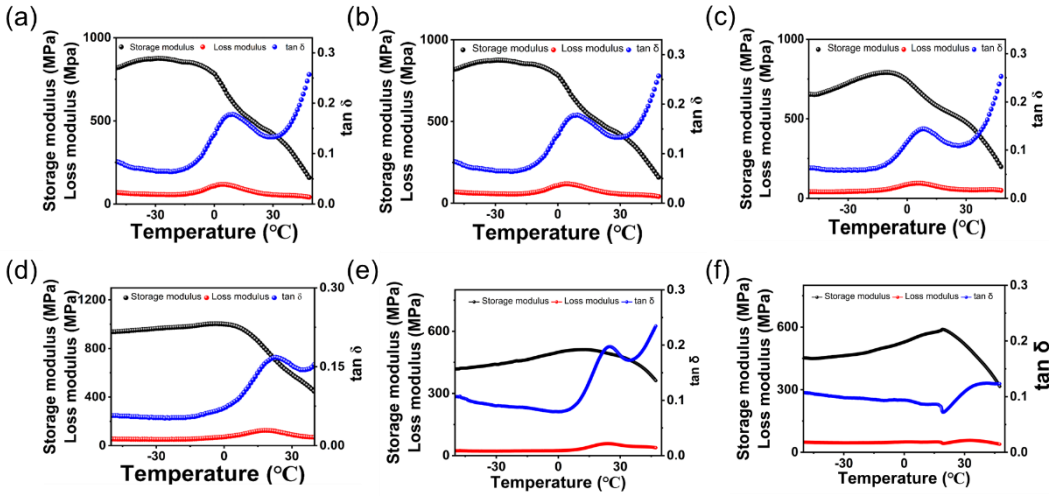

Figure S39. DMA tests of(a) poly[**TA-Ce**]; (b) poly[**TA-Sp**]; (c) poly[**TA-Ch**]; (d) poly[**TA-Gu**]; (e) poly[**TA-Cp**]; and (f) poly[**TA-Ps**].

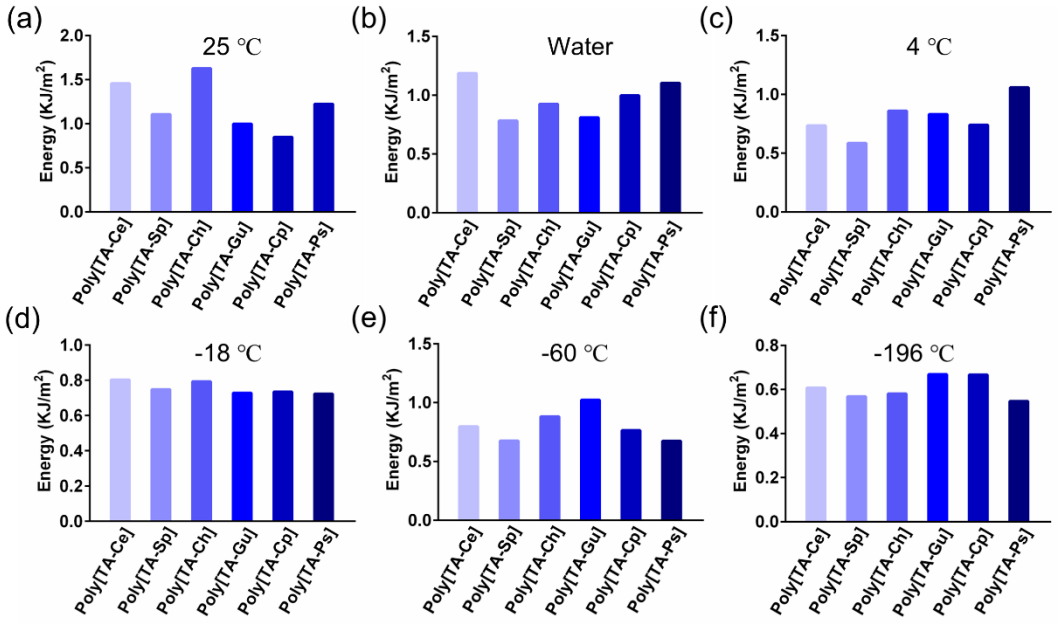

Figure 40. Impact resistance of poly[**TA-biomass**]s at different conditions. (**TA/biomass** = 10/1)

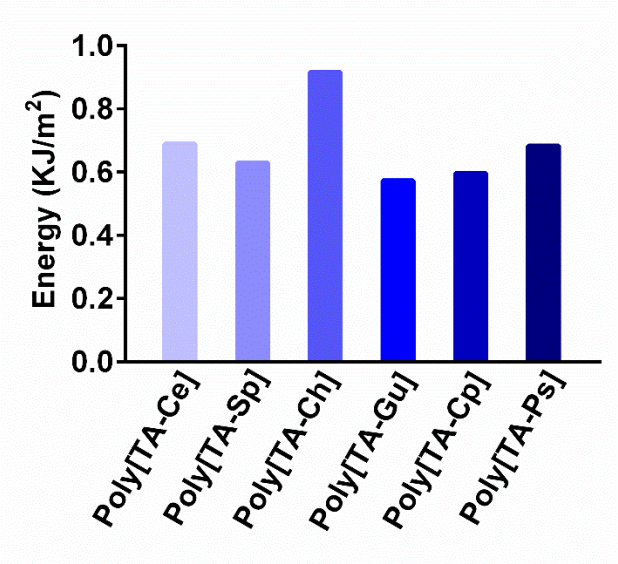

Figure S41. Impact resistance of poly[**TA-Ce**], poly[**TA-Sp**], poly[**TA-Ch**], poly[**TA-Gu**], poly[**TA-Cp**], and poly[**TA-Ps**] after reheating. (**TA**/**biomass** = 10/1)

9. The recyclability of poly[TA-biomass]s

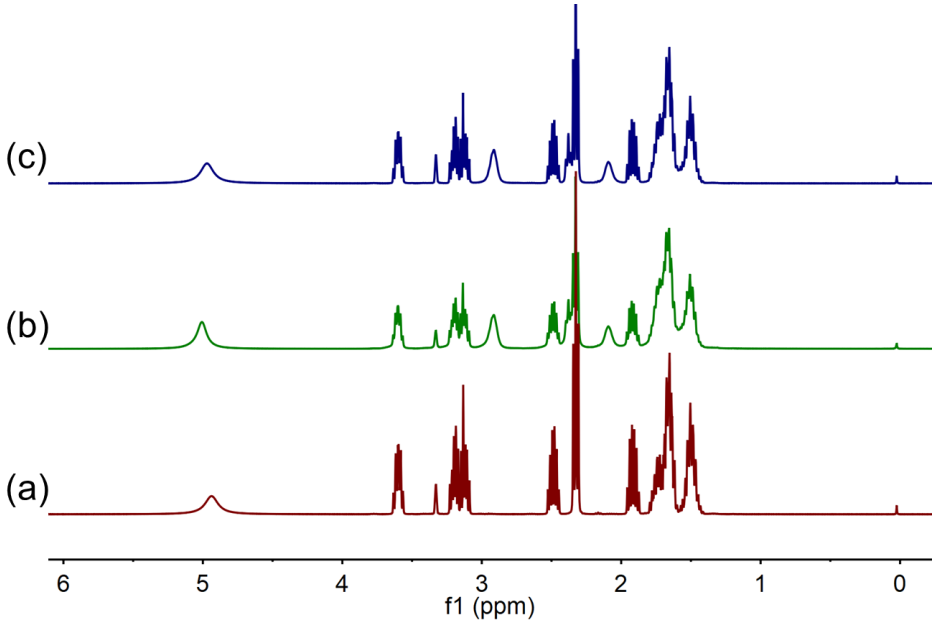

Figure S42. ^{1}H NMR (400 MHz, MeOH-d_4, room temperature): (a) **TA**, (b) recycled poly[**TA**] (from poly[**TA-Gu**]), and (c) poly[**TA**].

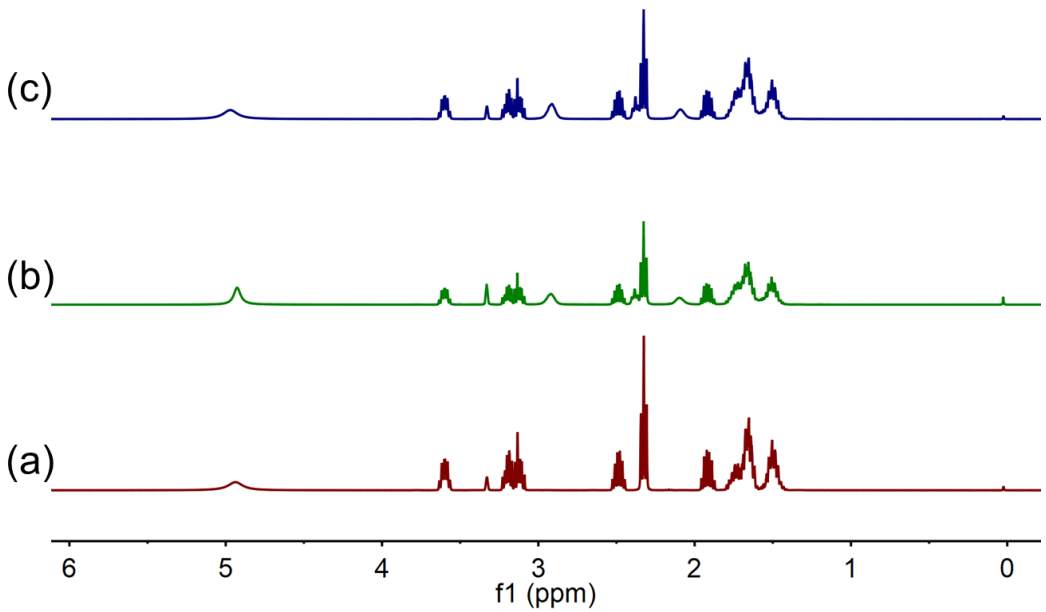

Figure S43. ^{1}H NMR (400 MHz, MeOH-d_4, room temperature): (a) **TA**, (b) recycled poly[**TA**] (from poly[**TA-Ps**]), and (c) poly[**TA**].

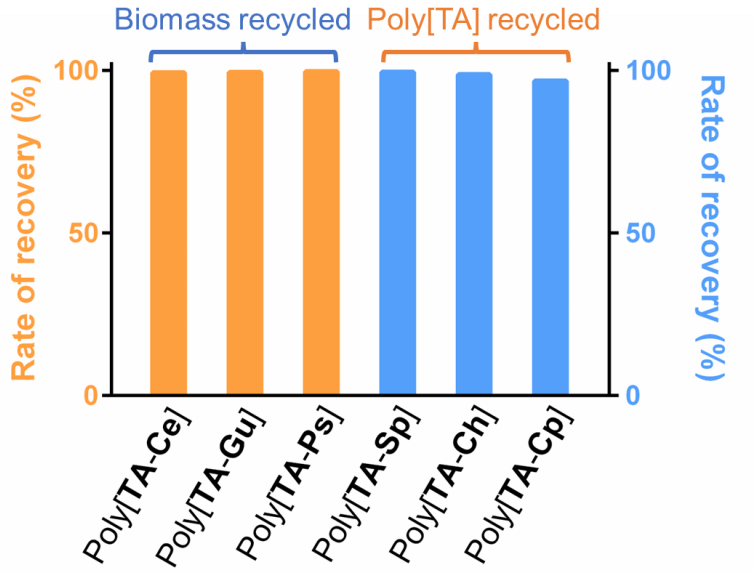

Figure S44. The recovery rates of poly[**TA-biomass**]s.

10. The biocompatibility and antibacterial properties of poly[TA-biomass]s

Cell culture

NIH 3T3 cells were cultured in standard DMEM (Gibco, 11965092) supplemented with 10% bovine growth serum (Gibco, 16030074) and 1% penicillin/streptomycin (Gibco,

15140122) at 37 °C with 5% CO_2.

Animals

C57/BL6 mice were purchased from the Chengdu Dossy Experimental Animals CO. LTD. After 1 week of adaptation, mice were randomly allocated into the Sham (NT) group and poly[**TA**] administration group and housed in specific pathogen-free facilities under a 12-h light and 12-h dark cycle. Temperature (23 ± 2 °C) and humidity (55%) were held constant in animal housing. For the administration group, power poly[**TA**] was mixed with the food with a dosage of 250 mg/ kg of the mice's body weight and 500 mg/ kg of the mice's body weight. All animals were allowed free access to food and clean water in the absence or presence of poly[**TA**]. Approvals for all the protocols were obtained from the Subcommittee on Research and Animal Care (SRAC) of Sichuan University.

Cell viability assay and Live/dead stain

The cytotoxicity of poly[**TA**] were evaluated by Cell Counting Kit-8 (CCK8, APExBIO) assay and live/dead cell staining kit (Beyotime Biotechnology). NIH-3T3 murine fibroblast cells (ACC no. 59, DSMZ, Braunschweig, Germany) cells were seeded into 96-well plates at a concentration of 104 cells per well. After 24 h incubation, the culture medium was removed and replaced with 100 μL of fresh medium containing PBS, poly[**TA**] with different concentrations. The cells were incubated for another 0, 24, and 72 h. Then, each well was replaced by 100 μL of fresh medium added with 10 μL of CCK-8 reagent. After 2 h of incubation, the optical density was measured at 450 nm by a Spectrophotometer (Thermo Fisher Scientific). The percentage of cell viability was calculated using the following equation:

Cell viability% = (A450, treated-x h – A450, blank)/(A450, treated-0 h – A450, blank) × 100%, where A450, treated-x h is the absorbance in the presence of tested compounds at a certain time point (24 and 72 h), A450, treated-0 h is the absorbance in the presence of tested compounds at 0 h, and A450, blank is the absorbance in the presence of PBS, respectively.

For the live/dead staining, cells were co-cultured in 96-well plates at a density of 2 ×

103 cells/well with different concentrations of poly[**TA**] (0 mg/mL, 0.01 mg/mL, 0.1 mg/mL, and 1 mg/mL) for 1 and 3 days respectively, after which 100 μL of live/dead staining solution (Calcein/PI Cell Activity Kit and Cytotoxicity Assay Kit) was added. Cells were then incubated in the dark at 37 °C for 30 min. The stained cells were observed using an inverted fluorescence microscope (IX73, one-deck system, OLYMPUS).

Hematoxylin and Eosin (H&E) Staining

After administration of poly[**TA**] for 3 weeks, mice were sacrificed and major organs (heart, liver, spleen, lung, and kidney) were fixed with 4% PFA for 24 h. After serial dehydration in a series of ethanol (70 – 100%), samples were embedded in paraffin. 5 μm sections were processed by a microtome (#RM2235, Leica) and ready for staining. Sections were stained using H&E stain kit (G1120, Solarbio) according to the manufacturer's instructions. The nuclei are stained purple, while the cytoplasmic components are pink. Images of stained sections were obtained by an optical microscope (BX53, Olympus).

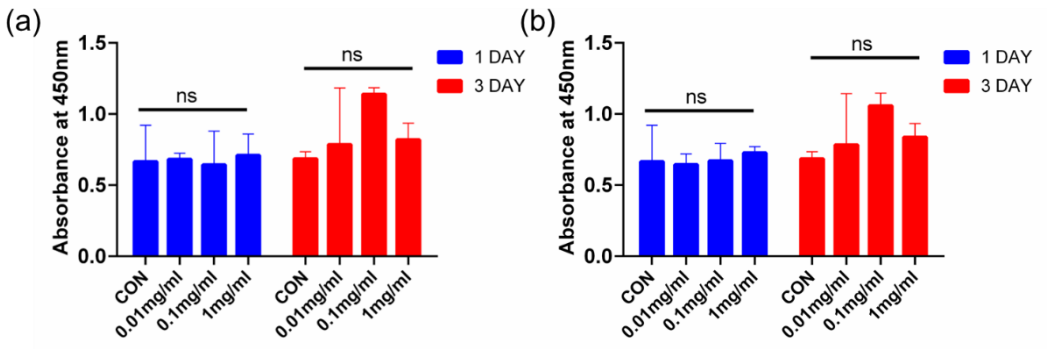

Figure S45. Cell viability of HUVECs cells co-cultured with (a) **TA** and (b) poly[**TA**] for 1, 3 days. All presented data are mean values ± SEM from the mean from n=3 independent measurements on independent samples. One-way ANOVA. (*P < 0.05, **P < 0.01, ***P <0.001, and "ns" denoted no significant difference)

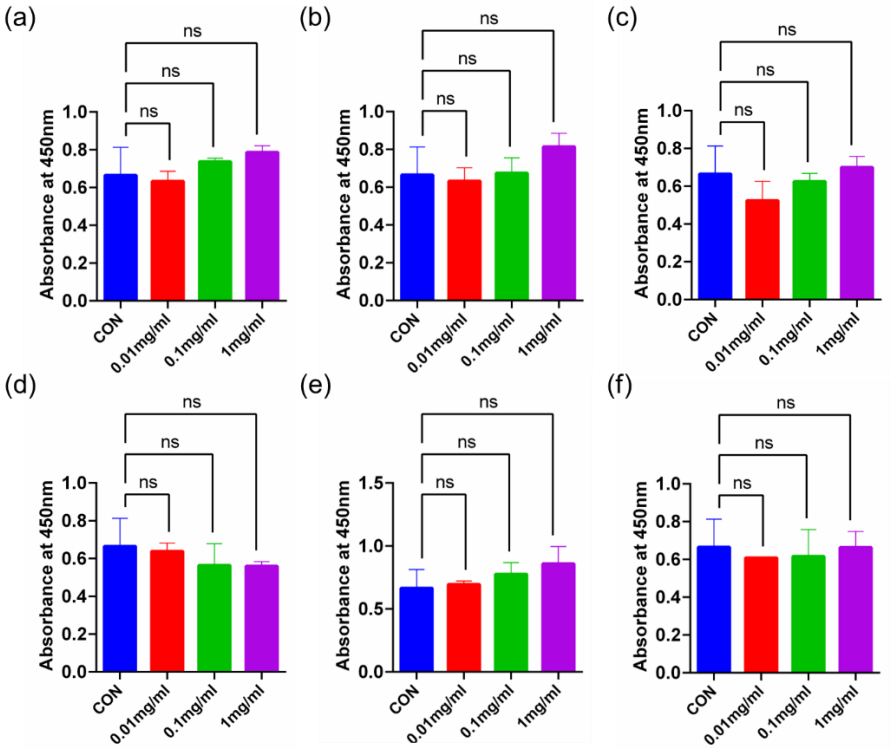

Figure S46. Cell viability of HUVECs cells co-cultured with (a) poly[**TA-Ce**]; (b) poly[**TA-Sp**]; (c) poly[**TA-Ch**]; (d) poly[**TA-Gu**]; (e) poly[**TA-Cp**]; and (f) poly[**TA-Ps**]. for 1 day. All presented data are mean values ± SEM from the mean from n=3 independent measurements on independent samples. One-way ANOVA. (*P < 0.05, **P < 0.01, ***P <0.001, and "ns" denoted no significant difference)

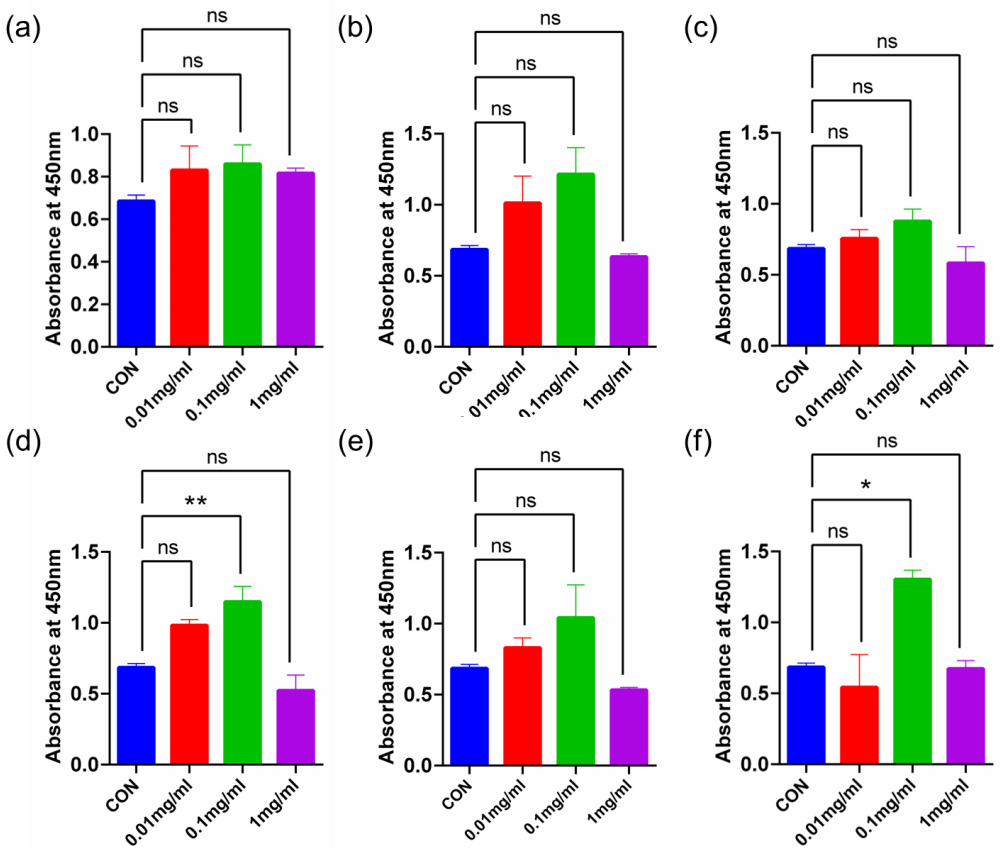

Figure S47. Cell viability of HUVECs cells co-cultured with (a) poly[**TA-Ce**]; (b) poly[**TA-Sp**]; (c) poly[**TA-Ch**]; (d) poly[**TA-Gu**]; (e) poly[**TA-Cp**]; and (f) poly[**TA-Ps**]. for 3 days. All presented data are mean values ± SEM from the mean from n=3 independent measurements on independent samples. One-way ANOVA. (*P < 0.05, **P < 0.01, ***P <0.001, and "ns" denoted no significant difference)

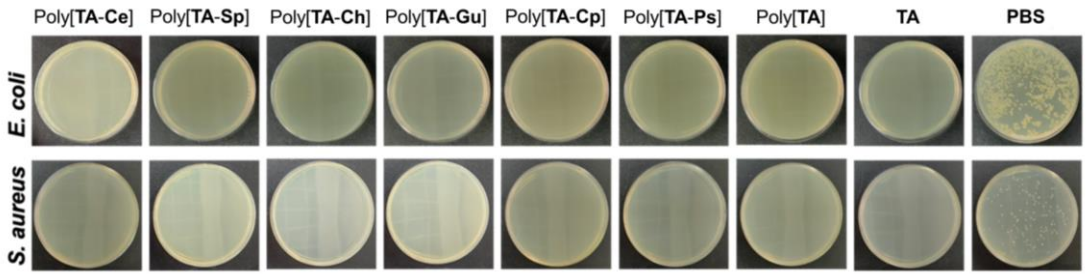

Figure S48. Typical photographs of the agar plate testing results of poly[**TA-biomass**]s with different additives against *E. coli* and *S. aureus*.

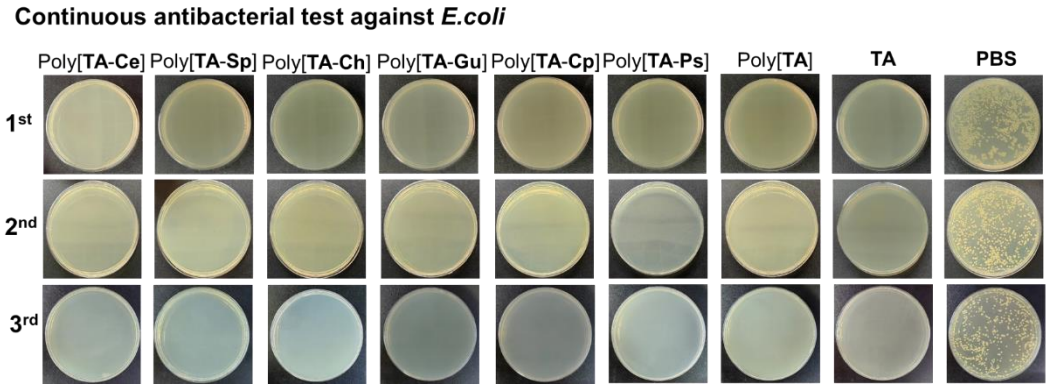

Figure S49. Typical photographs of the agar plate testing results of poly[**TA-biomass**]s with different additives against *E. coli* for three rounds of continuous antibacterial tests.

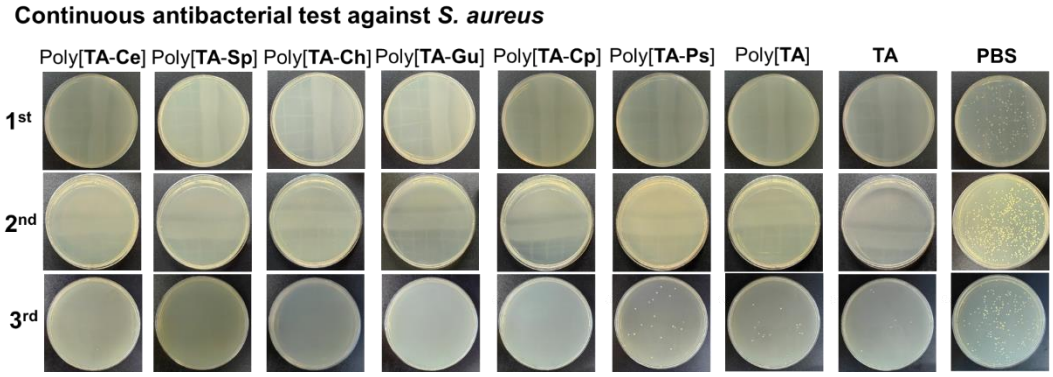

Figure S50. Typical photographs of the agar plate testing results of poly[**TA-biomass**]s with different additives against *S. aureus* for three rounds of continuous antibacterial tests.

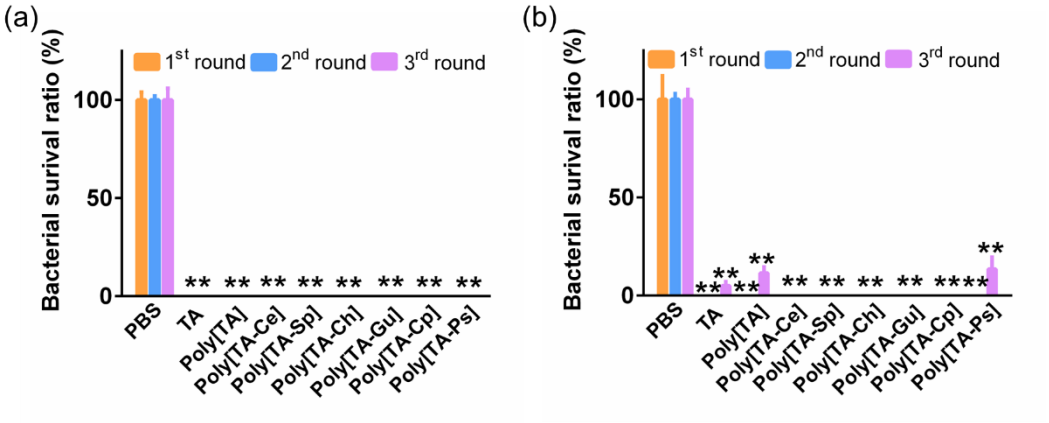

Figure S51. (a-b) Bacterial survival ration of *E. coli* and *S. aureus* after poly[**TA-biomass**]s with different additives against *E. coli* for three rounds of continuous antibacterial tests.

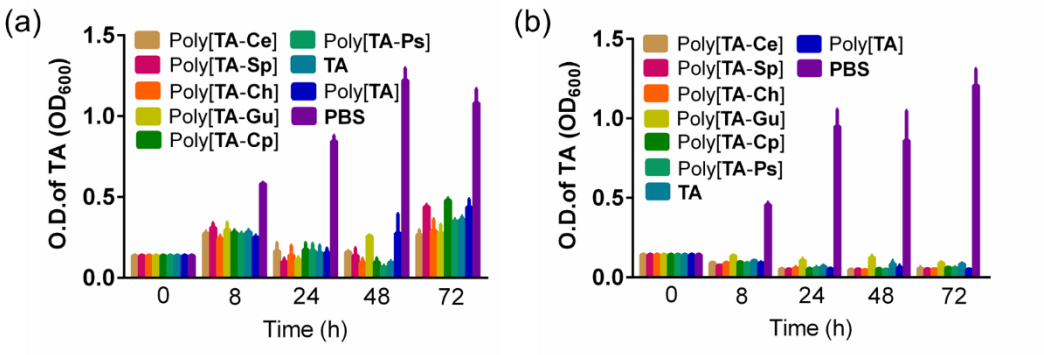

Figure S52. Bacterial growth of (a) *E. coli* and (b) *S. aureus* in the presence of poly[**TA-biomass**]s, poly[**TA**] and **TA** in 8 h, 24 h, 48 h and 72 h.

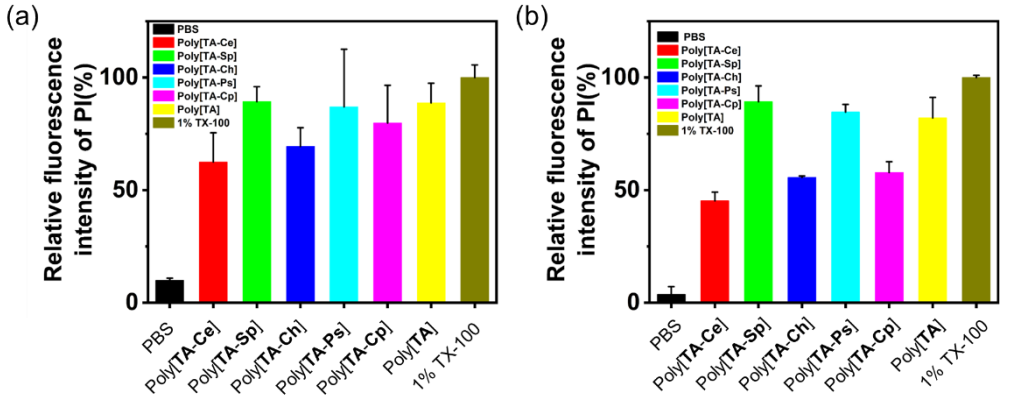

Figure S53. (a) PI uptake assay of (a) *E. coli* and (b) *S. aureus* with the treatment of PBS, poly[**TA-biomass**]s, and 1% TX-100 for 90 min, respectively.

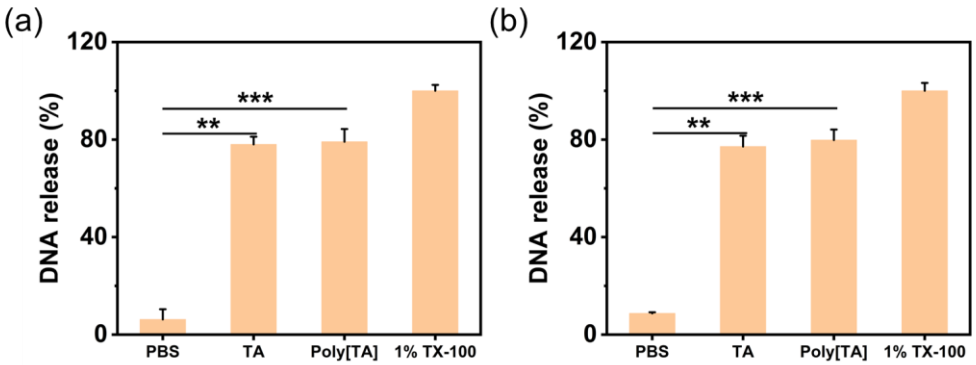

Figure S54. BCA protein assay of (a) *E. coli* and (b) *S. aureus* in the presence of PBS, **TA**, poly[**TA**] and 1% TX-100 for 90 min, respectively.

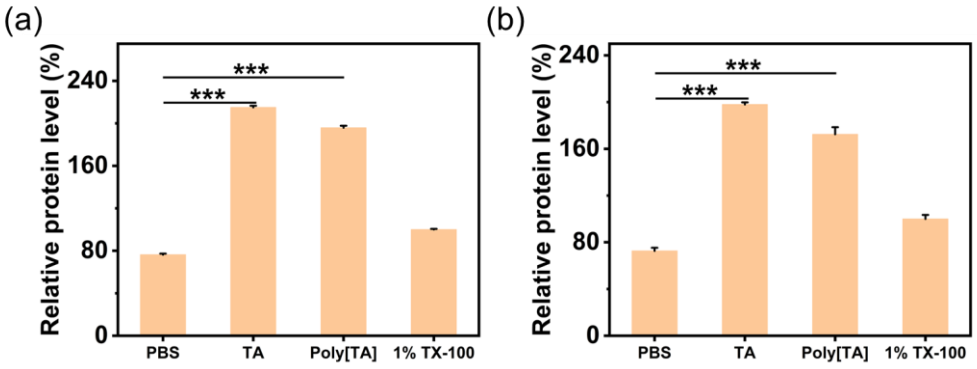

Figure S55. Nucleic acid leakage assay of (a) *E. coli* and (b) *S. aureus* with the treatment of PBS, **TA**, poly[**TA**] and 1% TX-100 for 90 min, respectively.

Propidium iodide (PI) uptake assay, BCA protein assay and nucleic acid leakage assay were carried out to gain insight into the possible antibacterial mechanism of these poly[**TA-biomass**]s. Similar to the results of bacteria treated with positive control, 1% Triton X-100 (1% TX-100), remarkable PI uptake can be observed in the *E. coli* and *S. aureus* suspensions incubated with poly[**TA-biomass**]s for 90 min (Figure S53), suggesting that the cell membrane integrities of *E. coli* and *S. aureus* were damaged with the treatment of poly[**TA-biomass**]s. BCA protein assay and nucleic acid leakage assay further reveal that **TA** powder and poly[**TA**] can cause the leakage of the intracellular proteins and larger macromolecules, e.g., DNA or RNA, which could be noted in Figure S54 and S55. These results indicate that poly[**TA-biomass**]s can significantly increase the permeability of bacterial cell membranes of *E. coli* and *S. aureus*, and further lead to the loss of intracellular substance, finally cause the bacterial cell death.

11. Videos

Video S1. Application of poly[**TA-Ce**] as a water pipe

Video S2. The **Ce** film was broken by a small external force

12. References

S1. C. Cai, S. Wu, Y. Zhang, F. Li, Z. Tan, and S. Dong, *Adv. Sci.*, 2022, **9**, 2203630.

S2. H. Wang, Y. Wang, W. Xu, H. Zhang, J. Lv, X. Wang, Z. Zheng, Y. Zhao, L. Yu, Q. Yuan, L. Yu, B. Zheng, and L. Gao, *ACS Appl. Mater. Interfaces*, 2023, **15**, 54266–54279.

S3. Q. Zhang, C.-Y. Shi, D.-H. Qu, Y.-T. Long, B. L. Feringa, H. Tian, *Sci. Adv.*, 2018, **4**, eaat8192.

S4. Q. Zhang, Y. Deng, C.-Y. Shi, B. L. Feringa, H. Tian, and D.-H. Qu, *Matter*, 2021, **4**, 1–13.

S5. W. Zheng, L. Xu, Y. Li, Y. Huang, B. Li, Z. Jiang, G. Gao, *J. Colloid Interface Sci.*, 2021, **599**, 360–369.

S6. K. Zhang, Z. Wang, J. Zhang, Y. Liu, C. Yan, T. Hu, C. Gao, Y. Wu, *Eur. Polym. J.*, 2021, **156**, 110618.

S7. K. Zhang, J. Zhang, Y. Liu, Z. Wang, C Yan, C Song, C. Gao, Y Wu, *J. Colloid Interface Sci.*, 2021, **594**, 584–592.

S8. Q. Zhang, Y.-X. Deng, H.-X. Luo, C.-Y. Shi, G. M. Geise, B. L. Feringa, H. Tian, and D.-H. Qu, *J. Am. Chem. Soc.*, 2019, **141**, 12804−12814.

S9. Y. Wang, S. Sun, and P. Wu, *Adv. Funct. Mater.*, 2021, **31**, 2101494.

S10. J. Chen, D. Guo, S. Liang, and Z. Liu, *Polym. Chem.*, 2020, **11**, 6670–6680.